

# Simulation of Axon Activation by Electrical Stimulation— Applying Alternating-Direction-Implicit Finite- Difference Time-Domain Method

Charles T. M. Choi<sup>1,2</sup> and Shu-Hai Sun<sup>1</sup>

<sup>1</sup>Department of Computer Science and Institute of Biomedical Engineering, National Chiao Tung University, Hsinchu 30010, Taiwan

<sup>2</sup>Department of Electrical Engineering, National Chiao Tung University, Hsinchu 30010, Taiwan

**In a typical approach to model electrical stimulation of an axon, a cable model equivalent to an axon was placed in a simple homogeneous medium. An electrode was used to induce an excitation to stimulate the cable model, and then the transmembrane potentials and the ionic currents in the cable model in temporal domain were observed. Unfortunately, this simulation approach is not realistic since inhomogeneous tissues near the axon is not considered. In this paper, the alternating-direction-implicit finite-difference time-domain (ADI-FDTD) method is coupled with the equivalent model of a membrane (the Hodgkin–Huxley model), and a novel simulation scheme is developed to predict axon activation. By testing axon activation with current excitation, the simulation results show the new method is useful for simulating axon activation.**

**Index Terms**—Alternating-direction-implicit finite-difference time-domain (ADI-FDTD), axon stimulation, cable model, Hodgkin–Huxley (HH) model.

## I. INTRODUCTION

**T**HE equivalent electric circuit representing the membrane of a squid giant axon was proposed by Hodgkin and Huxley [1]. The Hodgkin–Huxley (HH) model is useful for simulating the membrane activation when a current is injected into a squid giant axon. Although classical HH experiments were carried out on the giant squid axon, differences in external potentials caused by the thickness of the axon were neglected in the following studies. In 1976, McNeal first modeled an axon using many small axon segments described by the equivalent model of a membrane and then connected them with the resistances of the axoplasm [2]. This kind of cable model is useful for simulating and predicting the axon response to extracellular electric stimulation [3].

When simulating axon activation by using the cable model, the medium surrounding the cable model is assumed as simple or homogeneous tissue, and this assumption does not correspond to the realistic situation, where inhomogeneous mediums may be near the axon, or several kinds of tissues may surround the axon. This paper introduces using the finite-difference time-domain (FDTD) method [4] to simulate axon activation. In the FDTD method, the temporal and spatial domains are discretized, and the wave propagation can be simulated by computing the discrete electromagnetic field in the computational domain. Since the numerical accuracy is affected by the cell size, and the maximum temporal increment is limited by the Courant–Friedrich–Levy (CFL) stability condition, the simulation of an axon with a diameter of several micrometer requires enormous computation resources. By incorporating the alternating-direction-implicit (ADI) technique into FDTD,

the ADI-FDTD method becomes free of the CFL condition [5]–[14]. By coupling ADI-FDTD with the HH model, the space of axons is discretized by fine cells, the remainder is discretized by coarse cells, and the proposed method is able to simulate axon activation with large temporal increment to improve the efficiency. In this paper, simulation results of electrical stimulation of an unmyelinated axon placed in a homogeneous medium show the accuracy of the proposed method matches that of the conventional cable model.

## II. METHOD

In this section, the cable model is introduced first, followed by a description of the algorithm of the coupling ADI-FDTD method with the HH model.

### A. Cable Model

Hodgkin and Huxley gave a general description of the time course of the current which flows through the membrane of a squid giant axon when the potential difference across the membrane is suddenly changed from its steady state [1]. The results in [1] suggest that the behavior of a membrane may be represented by the electrical circuit as shown in Fig. 1(a). The current can be carried through the membrane either by charging the membrane capacitance or by movement of ions through the nonlinear conductance in parallel with the membrane capacitance. The equation that describes the HH model is

$$\begin{aligned} I &= I_{C_m} + I_K + I_{Na} + I_L \\ &= C_m dV_m/dt + g_K n^4 (V_m - V_K) \\ &\quad + g_{Na} m^3 h (V_m - V_{Na}) + g_L (V_m - V_L) \end{aligned} \quad (1)$$

where  $I$  is the total ionic current across the membrane due to the flux of ions,  $C_m$  is the membrane capacity per unit area,  $g_K$  and  $g_{Na}$  are the conductance of potassium and sodium channels,  $g_L$  is the leakage conductance of chloride or other, and  $V_m$  is the potential across the membrane. The parameters  $n$ ,  $m$ , and  $h$  in

Manuscript received July 08, 2011; revised October 05, 2011; accepted October 22, 2011. Date of current version January 25, 2012. Corresponding author: C. T. M. Choi (e-mail: c.t.choi@ieee.org).

Color versions of one or more of the figures in this paper are available online at <http://ieeexplore.ieee.org>.

Digital Object Identifier 10.1109/TMAG.2011.2175377

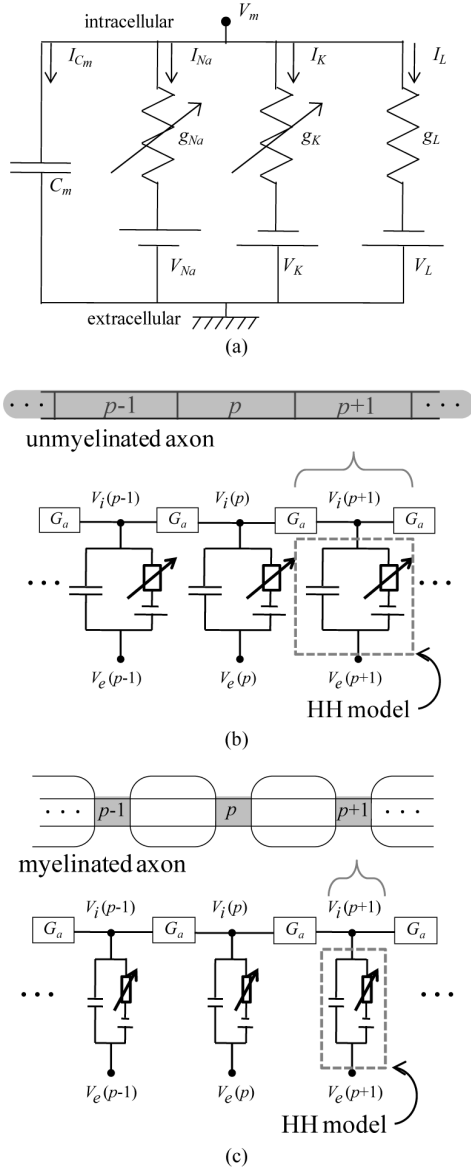


Fig. 1. Equivalent electric circuits of (a) a membrane, (b) an unmyelinated axon, and (c) a myelinated axon.

(1) are the probability parameters determining the percentage of open channels, and all variables are change between 0 and 1 as functions of time and voltage. More details about the HH model are described in [1].

As shown in Fig. 1(b) and (c), the cable models based on the HH model are represented by the electric network. Applying Kirchhoff's current law (a set of differential equations discrete in space and continuous in time, also known as the cable equation) to the electric network is useful for predicting axon activation [2], [3].

### B. ADI-FDTD Algorithm

For the FDTD method, Maxwell's curl equations are discretized in temporal and spatial domains, and the electric- and magnetic-field components are allocated on Yee cells filled the computational domain. It is useful for analyzing the distribution and the propagation of the electromagnetic field in the computational domain. By coupling the FDTD method with the ADI

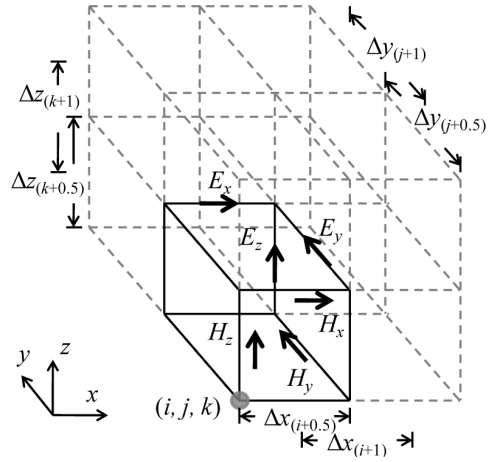


Fig. 2. Graded meshes in the 3-D domain.

technique, the ADI-FDTD method is free of the CFL condition. The process of updating electromagnetic-field components in a time step in the FDTD method is shown in published papers [12]. Here the electromagnetic-field components in Cartesian coordinate system are distributed in graded meshes as shown in Fig. 2, and the updated formulations of  $E_{zx}$  and  $H_{yx}$  components in the first half-time step are shown below as examples

$$\begin{aligned}
 E_{zx,(i,j,k+1/2)}^{n+1/2} &= ca_{x,(i,j,k+1/2)} E_{zx,(i,j,k+1/2)}^n + cb_{x,(i,j,k+1/2)} \\
 &\cdot (H_{yx,(i+1/2,j,k+1/2)}^{n+1/2} + H_{yz,(i+1/2,j,k+1/2)}^{n+1/2} \\
 &- H_{yx,(i-1/2,j,k+1/2)}^{n+1/2} - H_{yz,(i-1/2,j,k+1/2)}^{n+1/2}) \quad (2) \\
 H_{yx,(i+1/2,j,k+1/2)}^{n+1/2} &= da_{x,(i+1/2,j,k+1/2)} H_{yx,(i+1/2,j,k+1/2)}^{n+1/2} \\
 &+ db_{x,(i+1/2,j,k+1/2)} (E_{zx,(i+1,j,k+1/2)}^{n+1/2} \\
 &+ E_{zy,(i+1,j,k+1/2)}^{n+1/2} \\
 &- E_{zx,(i,j,k+1/2)}^{n+1/2} - E_{zy,(i,j,k+1/2)}^{n+1/2}) \quad (3)
 \end{aligned}$$

where the coefficients are

$$ca_{s,(i,j,k)} = (4\epsilon_0 - \sigma_{s,(i,j,k)}\Delta t)/(4\epsilon_0 + \sigma_{s,(i,j,k)}\Delta t) \quad (4)$$

$$cb_{s,(i,j,k)} = 2\Delta t/[\Delta s_{(i,j,k)}(4\epsilon_0 + \sigma_{s,(i,j,k)}\Delta t)] \quad (5)$$

$$da_{s,(i,j,k)} = (4\mu_0 - \sigma_{s,(i,j,k)}\eta_0^2\Delta t)/(4\mu_0 + \sigma_{s,(i,j,k)}\eta_0^2\Delta t) \quad (6)$$

$$db_{s,(i,j,k)} = 2\Delta t/[\Delta s_{(i,j,k)}(4\mu_0 + \sigma_{s,(i,j,k)}\eta_0^2\Delta t)]. \quad (7)$$

The implicit formulations in these half-time steps can be solved with a tridiagonal matrix [9].

The FDTD method was extended to solve the distributed electromagnetic system with lumped elements and voltage and current sources [15]. Here the ADI-FDTD method is coupled with the equivalent electric current of the membrane (the HH model). If the definition of the current direction in (1) is the same as the direction of electric-field components in the ADI-FDTD method, (2) is modified as:

$$\begin{aligned}
 E_{zx,(i,j,k+1/2)}^{n+1/2} &= ca'_{x,(i,j,k+1/2)} E_{zx,(i,j,k+1/2)}^n + cb'_{x,(i,j,k+1/2)}
 \end{aligned}$$

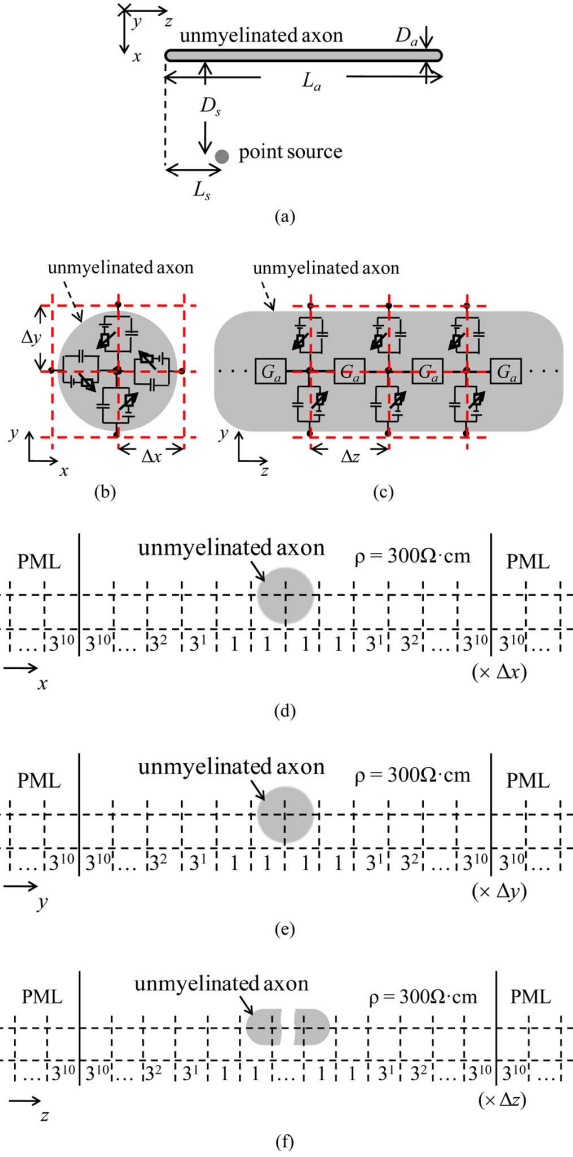


Fig. 3. (a) A simulated domain with an unmyelinated axon and a point source, the spatial discretization near the axon in (b)  $xy$  and (c)  $yz$  domains, and the cell distribution in (d)  $x$ , (e)  $y$ , and (f)  $z$  direction.

$$\begin{aligned}
 & \cdot (H_{yx,(i+1/2,j,k+1/2)}^{n+1/2} + H_{yz,(i+1/2,j,k+1/2)}^{n+1/2}) \\
 & - H_{yx,(i-1/2,j,k+1/2)}^{n+1/2} \\
 & - H_{yz,(i-1/2,j,k+1/2)}^{n+1/2} \\
 & + g_K n^4 V_K + g_{Na} m^3 h V_{Na} + g_L V_L)
 \end{aligned} \quad (7)$$

where the modified coefficients are

$$\begin{aligned}
 cd'_{s,(i,j,k)} &= [4C_m - \Delta t(g_K n^4 + g_{Na} m^3 h + g_L)] \\
 & \cdot [4C_m + \Delta t(g_K n^4 + g_{Na} m^3 h + g_L)]^{-1}
 \end{aligned} \quad (8)$$

$$\begin{aligned}
 cb'_{s,(i,j,k)} &= 2\Delta t \cdot \{\Delta s_{(i,j,k)}[4\epsilon_0 + \Delta t \\
 & \cdot (g_K n^4 + g_{Na} m^3 h + g_L)]\}^{-1}
 \end{aligned} \quad (9)$$

### III. SIMULATION RESULT

As shown in Fig. 3(a), an unmyelinated axon with an interior resistivity of  $34.5 \Omega \cdot \text{cm}$  placed in a homogeneous medium

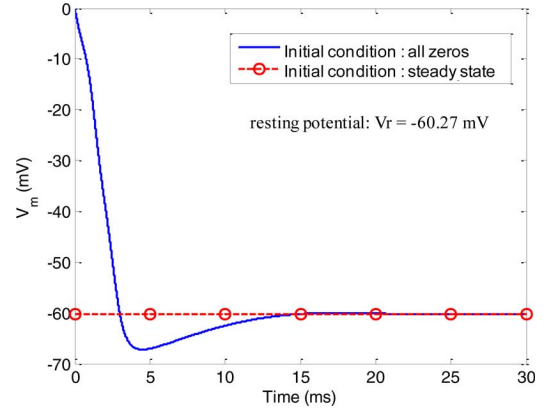


Fig. 4. Convergence of the membrane potential.

TABLE I  
INITIAL CONDITIONS OF THE MEMBRANE FOR CONVERGENCE TEST

Initial condition	$V_m$ (mV)	$n$	$m$	$h$
all zeros	0	0	0	0
steady state	-60.27	0.3177	0.0529	0.5961

with the electrical resistivity of  $300 \Omega \cdot \text{cm}$  is simulated by the ADI-FDTD method coupled with the HH model, and the discretization of the computational domain is also shown in Fig. 3. The setting of the parameters shown in Fig. 3 is:  $D_a = 0.1$  mm;  $L_a = 7.5$  mm;  $D_s = 1$  mm;  $L_s = 1.5$  mm;  $\Delta x = \Delta y = 50 \mu\text{m}$ ; and  $\Delta z = 0.5$  mm. In each direction, the minimum cell is used to discretize the central area, and the cell whose size is gradually increased is used to discretize the outer area. The maximum cell size is  $3^{10}$  times of the minimum cell size, and ten layers of perfect match layer (PML) are used in this simulation. The convergence test and the stimulation test are simulated to verify the performance of the ADI-FDTD method coupled with the HH model.

#### A. Convergence Test

Under the steady-state conditions, the voltage across the membrane is equal to the voltage of the resting potential  $V_r$ , where the voltage of the resting potential can be analytically computed as follows:

$$V_r = \frac{g_K n^4 V_K + g_{Na} m^3 h V_{Na} + g_L V_L}{g_K n^4 + g_{Na} m^3 h + g_L} = -60.27 \text{ mV}. \quad (10)$$

In order to reduce the computational time, the initial temporal increment is set as 0.117 ps and increases at the rate of 1.01 times per time step until the temporal increment is larger than 5.878 ns, which is about  $5 \times 10^4$  times of the temporal increment under the CFL stability condition. Two initial conditions of the membrane are considered: all zeros and steady states. The values of the parameters setting in the initial conditions are listed in Table I, and the simulation results are shown in Fig. 4. From the simulation results, it was found that the membrane potential converges to the resting potential when the initial conditions of the membrane are all zeros, and the membrane potential maintains at the resting potential when the initial conditions of the membrane are set as steady-state

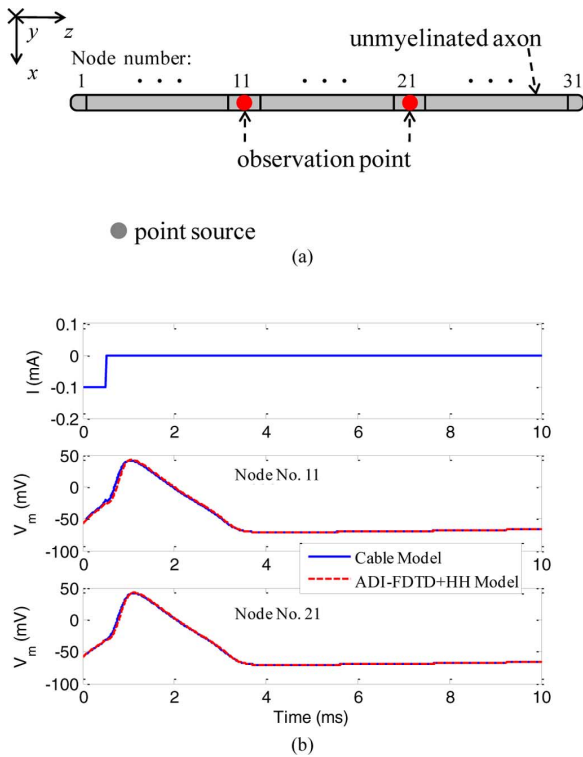


Fig. 5. (a) Locations of the observation points. (b) Pulse of the current induced at the point source and the membrane potentials at nodes no. 11 and no. 21.

values. Therefore, by coupling ADI-FDTD method with the HH model, this proposed method retains the characteristic of the HH model.

### B. Stimulation Test

After finishing the convergence test, the point source induces a pulse with amplitude of  $-100 \mu\text{A}$  and a pulse width of  $500 \mu\text{s}$ . As shown in Fig. 5(a), the observation points located at nodes number 11 and number 21 are used to observe the membrane potential. The stimulation current and the membrane potentials at the observation points are shown in Fig. 5(b). By comparing the simulation results from the proposed method with those from the cable model, the membrane potential simulated by the proposed method matches the simulation results of the conventional method. The proposed method is demonstrated to have achieved a good performance in simulating the characteristic of unmyelinated axon activation by electrical stimulation.

## IV. CONCLUSION

By coupling the ADI-FDTD method with the HH model, a novel method is presented to model the activation of a membrane and the propagation of a spike in an unmyelinated axon. The simulation results showed that this method retains the characteristic of the HH model, and it is useful for simulating axon

activation and the propagation of a spike in an unmyelinated axon. Although the simulation results of a myelinated axon are not shown in this paper, by the similar manner to discretize the space near a myelinated axon and couple ADI-FDTD with the electric network of myelinated axon, the proposed method can also simulate the activation of a myelinated axon.

## ACKNOWLEDGMENT

This work was supported in part by National Science Council, Taiwan, under Grant 98-2221-E-009-089 MY3, Grant 99-2321-B-009-001, and Grant 100-2321-B-009-002.

## REFERENCES

- [1] A. L. Hodgkin and A. F. Huxley, "A quantitative description of membrane current and its application to conduction and excitation in nerve," *J. Physiol. (Lond.)*, vol. 117, pp. 500–544, 1952.
- [2] D. R. McNeal, "Analysis of a model for excitation of myelinated nerve," *IEEE Trans. Biomed. Eng.*, vol. BME-23, pp. 329–337, Jul. 1976.
- [3] F. Rattay, "Analysis of models for external stimulation of axons," *IEEE Trans. Biomed. Eng.*, vol. BME-33, no. 10, pp. 974–977, Oct. 1986.
- [4] K. S. Yee, "Numerical solutions of initial boundary value problems involving Maxwell's equations in isotropic media," *IEEE Trans. Antennas Propag.*, vol. 14, no. 3, pp. 302–307, May 1966.
- [5] M. Darms, R. Schuhmann, H. Spachmann, and T. Weiland, "Dispersion and asymmetry effects of ADI-FDTD," *IEEE Microw. Wireless Compon. Lett.*, vol. 12, no. 12, pp. 491–493, Dec. 2002.
- [6] G. Sun and C. W. Trueman, "Unconditionally stable Crank-Nicolson scheme for solving two-dimensional Maxwell's equations," *Electron. Lett.*, vol. 39, no. 7, pp. 595–597, 2003.
- [7] S. W. Staker, C. L. Holloway, A. U. Bhoobe, and M. Piket-May, "Alternating-direction implicit (ADI) formulation of the finite-difference time-domain (FDTD) method: Algorithm and material dispersion implementation," *IEEE Trans. Electromagn. Compat.*, vol. 45, no. 2, pp. 156–166, May 2003.
- [8] N. V. Kantartzis, T. T. Zygiridis, and T. D. Tsiouboukis, "An unconditionally stable higher-order ADI-FDTD technique for the dispersionless analysis of generalized 3-D EMC structures," *IEEE Trans. Magn.*, vol. 40, no. 2, pp. 1436–1439, Mar. 2004.
- [9] C. T. M. Choi and S.-H. Sun, "Numerical performance and applications of the envelope ADI-FDTD method," *IEEE Trans. Microw. Theory Tech.*, vol. 54, no. 1, pp. 256–264, Jan. 2006.
- [10] W. Fu and E. L. Tan, "A parameter optimized ADI-FDTD method based on the (2,4) stencil," *IEEE Trans. Antennas Propag.*, vol. 54, no. 6, pp. 1836–1842, Jun. 2006.
- [11] D. L. Sounas, N. V. Kantartzis, and T. D. Tsiouboukis, "Optimized ADI-FDTD analysis of circularly polarized microstrip and dielectric resonator antennas," *IEEE Microw. Wireless Compon. Lett.*, vol. 16, no. 2, pp. 63–65, Feb. 2006.
- [12] S.-H. Sun and C. T. M. Choi, "Envelope ADI-FDTD method and its application in three-dimensional nonuniform meshes," *IEEE Microw. Wireless Compon. Lett.*, vol. 17, no. 4, pp. 253–255, Apr. 2007.
- [13] W. Fu and E. L. Tan, "Stability and dispersion analysis for ADI-FDTD method in lossy media," *IEEE Trans. Antennas Propag.*, vol. 55, no. 4, pp. 1095–1102, Apr. 2007.
- [14] Y. Zhang and S.-W. Lu, "Genetic algorithm in reduction of numerical dispersion of 3-D alternating-direction-implicit finite-difference time-domain method," *IEEE Trans. Microw. Theory Tech.*, vol. 55, no. 5, pp. 966–973, May 2007.
- [15] W. Sui, D. A. Christensen, and C. H. Durney, "Extending the two-dimensional FDTD method to hybrid electromagnetic systems with active and passive lumped elements," *IEEE Trans. Microw. Theory Tech.*, vol. 40, no. 4, pp. 724–730, Apr. 1992.